

Real World Operation of a Standard Lawn Mower Engine from a Scientific Perspective

Hermann Edtmayer, Alexander Trattner, Stephan Schmidt, Roland Kirchberger

Graz University of Technology, Institute for Internal Combustion Engines and Thermodynamics

Jakob Trentini, Johann Weiglhofer

Viking GmbH

Copyright © 2013 SAE Japan and Copyright © 2013 SAE International

ABSTRACT

This paper introduces a research project on a spark ignition engine used in non-road applications. The aim is to illustrate the present situation as basis for comparison. Furthermore to identify possible improvement potential in terms of performance, efficiency or exhaust and noise emissions.

The study is carried out in two steps. First a standard walk-behind lawn mower is equipped with measuring instrumentation for recording the cutting forces and the engine variables during real world operation. The tests are carried out on three different lawn types and two different blade types are investigated. Consequently, in a second step the engine is analysed on the engine test bench in stationary and transient operating mode. A complete engine mapping is done regarding all relevant variables. Additionally to the outdoor tests, fuel consumption and engine out emissions are measured on the engine dynamometer. The recorded data enables a detailed analysis of the engine behaviour. Furthermore the load spectrum during real world operation is diagrammed and the most frequent load and speed points of the engine on the different lawn types are identified. Moreover the flyweight governor system and, closely connected with it, the carburettor behaviour of the engine is observed under transient conditions.

INTRODUCTION

At the present time combustion engine operated working tools are part of the daily routine. They are deployed in private households, the agriculture sector, the construction industry and the professional gardening business. Conventional four stroke spark ignition engines operated with carburettor are the most frequently applied types therein. Such engines fulfil current emission legislations and average customer demands regarding performance and fuel consumption. Nevertheless, the question arises whether future requirements can be met and if there are possibilities to create new customer incentives. At the one hand it can be expected that the legislation situation will change in the

future. At the other hand the working tool market is highly competitive, thus it is essential to companies to provide novel customer benefits. Arguments for this, amongst other facts, are that there is a desire for strong and powerful and at the same time more efficient engines, giving evidence of an increasing environmental awareness. The question is if it's possible to transfer technology like injection systems, ECU and EMS into ICE units mentioned above, facing well known obstacles like system costs, packaging and durability demands, tool weight, etc.

Preliminary investigations are needed to determine and assess the actual circumstances for providing benchmark data and to locate possible improvement potential. In this context the research group is taking a closer look at a 180cm³ lawnmower engine in real world tests as well as on the engine test bench.

ENGINE AND APPLICATION

INVESTIGATED ENGINE

The object of investigation is a four stroke spark ignition engine built by Kawasaki. There are some good reasons for choosing this engine. First within its engine class it boasts sophisticated emission levels. Also the technical status is well developed. A steel camshaft is used and a circular lubrication system applied. This leads to a long life span of the engine.

In Table 1 the main technical specifications are listed. The engine shows a displacement of 179 cm³, one cylinder and a compression ratio of 8.5 to 1. The two overhead valves are actuated by push rods and rocker arms. The camshaft is located in the crank housing and propelled by a one stage gear drive. An automatic compression reduction system for the engine start is driven directly by the camshaft gear drive. The cylinder is orientated horizontally with a vertical crankshaft position. The engine is air cooled with the fan placed on top of it, directly attached to the flywheel.

Table 1: Kawasaki FJ180V STD engine specifications [1]

Engine Type	Forced Air-Cooled 4-cycle Vertical Shaft OHV Gasoline Engine
Number of cylinders	1
Bore x Stroke	65 x 54 mm
Displacement	179 cm ³
Compression ratio	8.5 : 1
Maximum power	3.4 kW (4.5 hp) / 3600 rpm
Maximum torque	10 Nm / 2400 rpm
Mixture preparation	Float type carburettor
Ignition	Flywheel magneto with CDI
Lubrication system	Circular lubrication
Oil capacity	0.6 l
Dry weight	17 kg
Emission aftertreatment	-

A baffle plate is guiding the flow pattern of the cooling air around the engine. As ignition system a flywheel magneto system with CDI is used. It is a non-variable type, thus the ignition timing is fixed to a specific crank angle position. A cross flow float type carburettor with fixed jet is deployed for mixture preparation. The circular lubrication system is driven by a positive displacement pump which provides the oil pressure feed. Within the exhaust a two stage silencer is applied, and no exhaust gas after treatment is installed. For starting the engine, a recoil system is used.



Figure 1: Kawasaki FJ180V STD [1]

Due to differing noise legislations in the European market as compared to the US market [2] [3], the speed of the cutting blade of the lawnmower has to be lowered. Therefore the high idle speed of the engine is downshifted from 3200 rpm to 2800 rpm. As a consequence a different carburettor needs to be installed to adjust the engine setup. In Figure 2 the engine output for the European setup is presented.

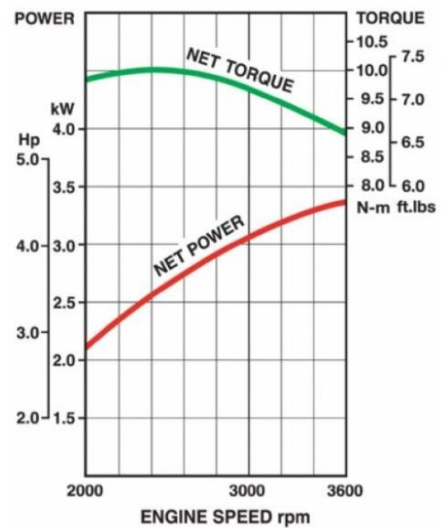


Figure 2: Kawasaki FJ180V STD output graph [1]

Mechanical flyweight governor

General purpose engines like the one at hand usually run at constant operating speed. Therefore a controller is needed to control the engine torque output for constant engine speed [4]. This application uses a simple mechanical flyweight all speed governor system that operates the throttle valve [5]. The high idle speed of the engine is set to a certain value through the carburettor settings. During operation a changing load requires a movement of the throttle flap to adapt the engine torque output. A decline in the engine speed due to a rising load causes the flyweight system (1) to operate a control shaft (2). Through a pushrod (3) and spring (4) mechanism this shaft is connected to the carburettor flap (5). This movement causes the flap to open.

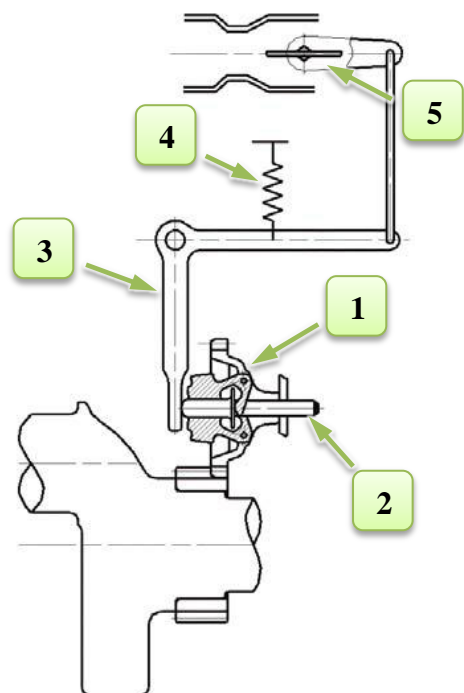


Figure 3: Sketch of a mechanical flyweight governor system [4]

LAWNMOWER: VIKING MB750 KS

The engine application investigated is a walk behind lawnmower manufactured by Viking GmbH, which is shown in Figure 4. It is designed for professional use and provides a travel drive with 3-speed transmission. A blade clutch allows for turning off the mowing operation. For the investigations the blade clutch is removed in order to give space for the torque measuring flange. This should be explained in detail later on. The blade of 53 cm cutting width is surrounded by a cast aluminium housing. A cutting height adjustment is also implemented.



Figure 4: Lawnmower Viking MB750KS [6]

REAL WORLD TESTS

The aim of the first phase of the investigations is to capture data of the real world behaviour and hence the load spectrum of the lawnmower and the implemented engine. The tool is equipped with measurement instrumentation for recording the cutting forces and the main engine parameters, (explained in the next section). The values are logged during real world operation on three common lawn types (turf lawn, farm grassland and high meadow) which are available at the test area of Viking GmbH. Moreover there were two different blade types used (wing-blade, mulching-blade). For powering the measurement instrumentation a mobile ICE power supply is used. The measured data is captured with a portable data logger system.

PREPARATION DATA ACQUISITION

Measurement categories

The different measurement categories for capturing the required information are listed below.

1. Data logger

A portable data logger with high accuracy is used for recording the measured data.

Resolution: 16, 22 or 24 bit
Sampling rate: 100 kS/s to 1 MS/s per channel
Manufacturer: Dewetron

2. Engine torque / cutting force:

The engine torque is measured via a torque measuring flange which is a design by Viking GmbH. It consists of a rolling bearing system for providing minimal friction losses. The flange is shown in Figure 5. It is pivoted between the aluminium housing and the engine mount. A load cell, hinged on both sides, is tapping the cutting force.

Maximum measuring load: 200 N
Accuracy class: 0.05
Relative sensitivity error: $\pm 0.25\%$
Manufacturer: HBM (S2)

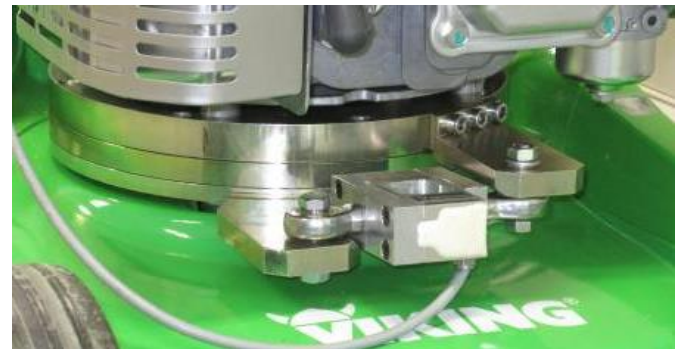


Figure 5: Torque measuring flange on the lawnmower

3. Engine speed:

A magnetic pickup sensor is scanning a 60 minus 2 toothed steel ring which is attached to the flywheel.

Manufacturer: TSI / RS components (RS285-756)

4. Cylinder pressure:

For the cylinder pressure indication a piezoelectric high temperature resistant sensor is mounted in the cylinder head. The sensor is installed with front sealing in an M5 x 0.5 bore.

Measuring range: 0 – 250 bar
Linearity: $\pm 0.3\%$ / FSO
Sensitivity: -20 pC / bar $\pm 0.5\%$
Operating temperature range: -20 – 350 °C
Natural frequency (measuring element): 160 kHz
Manufacturer: Kistler GmbH (6052C)

5. Lambda:

A high-precision lambda meter with sensor heating is used for detecting the Lambda value. The broad-band lambda probe is positioned in the inner chamber of the exhaust muffler.

Exhaust gas temperature range: $< 930\text{ °C}$
Accuracy at lambda 0.8: 0.80 ± 0.01
Manufacturer lambda probe: Bosch (LSU 4.9)
Measuring accuracy: $\pm 1.5\%$
Manufacturer lambda meter: Etas (LA4)

6. Throttle position:

To detect the position of the throttle flap, an angular position sensor is mounted to an extension of the throttle flap axis.

Linearity: $\pm 2\%$

Manufacturer: Murata (SV01L103AEA11T00)

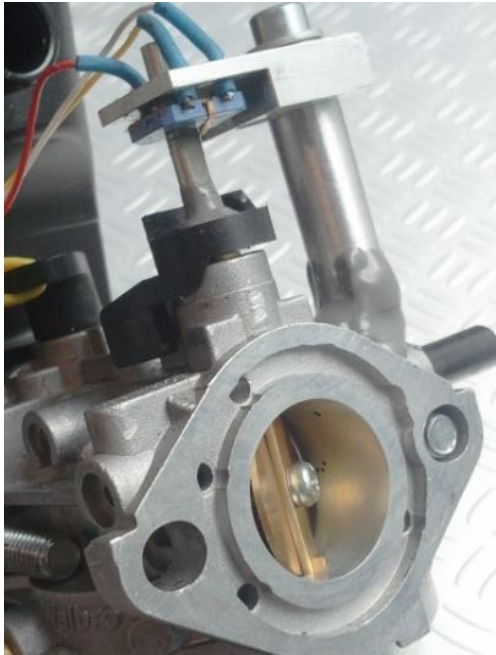


Figure 6: Throttle position pickup on the carburettor flap

7. Spark plug temperature:

A ring-shaped thermocouple type k sensor is used to detect the engine temperature at the spark plug seat.

Type K (NiCr / Ni)

Class 2: $\pm 2.2\text{ }^{\circ}\text{C}$ or $\pm 0.0075 * t$

Manufacturer: RS components

Out of the measurement data a variety of additional combustion parameters are calculated. This is been done via engine process calculation which is implemented in the data logger software.



Figure 7: Measurement setup of the lawnmower for the real world tests

EXPERIMENTS ON TEST AREA

The real world experiments are performed on the test area of Viking GmbH. Three different lawn types represent principal possible load conditions on the mower. The investigations are carried out with a variety of driving speeds and cutting heights. In addition there are two different cutting knives compared. A standard wing knife for mowing with catch basket and a mulching blade for a fertilisation of the lawn. Measurement durations are depending on the lawn sample length and vary between 10 and 50 seconds. At each lawn type, a couple of test runs are made to obtain reliable average data. After each run, the data is analysed to control the recorded data quality and to adapt the test settings if needed. As a result of the high resolution of the data logger, it is possible to clarify directly at the test area if the measured data is plausible or not.

Lawn types

The following lawn types are available on the test area for the investigations.

1. Turf lawn

The turf lawn, as can be seen in Figure 8, is a standard lawn type for private gardens or sports facilities. In the test facility it is about 10 cm high and of high density. The grass mainly consists of leaves and almost no straws. The density partially varies along the sample length.



Figure 8: Turf lawn with a 5 cm cut

2. Farm grassland

Farm grassland is a classic meadow within a height of about 20 cm mainly consisting of clay and a few different types of herbage. This type of grassland can not only be found on agricultural land but also on public areas like parks and green areas in towns. Its density is lower than the turf lawn's. Moreover the grass blades are longer and the grass stems are thicker and coarser.



Figure 9: Farm grassland

3. High meadow.

The third lawn type is an uncultivated high meadow of about 50 cm height containing different types of weed. The grass blades and stems are the strongest and hardest of all three types. It should represent the highest possible load conditions for this type of lawnmower.



Figure 10: High meadow

Blade types

In the field tests two different types of cutting blades are used. The wing blade is the standard blade for mowing. Wing flaps on the blade tips provide the transport of the grass into the catch basket.



Figure 11: Wing blade



Figure 12: Mulching blade in lawnmower

The mulching blade is used to fine-cut the lawn trimmings for a fertilization of the lawn. As can be seen in Figure 12, a second blade is attached to the system for the additional cut of the grass. The black insert at the left side of the housing is closing the grass throw-out channel as no grass box is used.

RESULTS OF THE REAL WORLD TEST

The recording resolution of the data logger system is set to 1 °CA. This results in a sampling rate of 18 kHz at an engine speed of 3000 rpm. Each data point presented in the graph represents an averaged value over the period of 720 °CA respectively two engine revolutions. Although the track length is varying between the single tests, each of the graphs is formatted to the same scaling. The intention is to depict the results more comparable for this publication. Because of packaging reasons the originally applied blade clutch has to be removed when installing the torque measurement flange. This leads to a slightly lower rotational inertia of the whole drivetrain but should only have a small influence on the measured values in highly transient operation.

Turf lawn 10 cm, 3rd gear, 5 cm cutting height:

The experiment is carried out with the fastest driving gear and medium cutting height. In Figure 13 and Figure 14 the first graph represents the course of the cutting torque in Nm, the second graph the engine speed in rpm and the third graph the throttle position in %. The axis of abscissas is showing the time in seconds. To capture the complete length of the experiment, the graph is split in two parts.

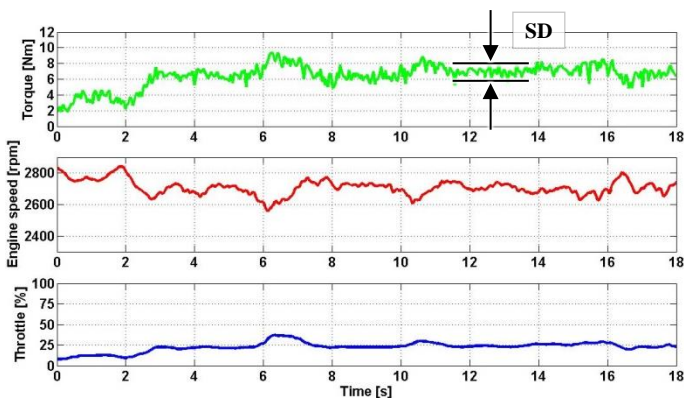


Figure 13: Cutting torque, engine speed and throttle position on turf lawn, first part

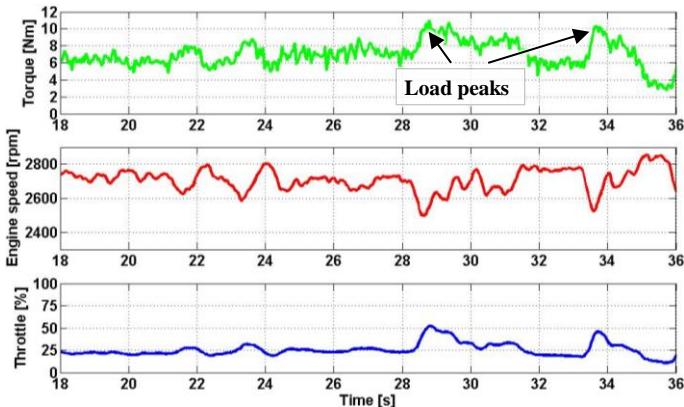


Figure 14: Cutting torque, engine speed and throttle position on turf lawn, second part

The high frequency torque shift, displayed through the flickering of the torque graph and its standard deviation (SD), shows the degree of constancy of the cutting force. Thus conclusions concerning the lawn density can be drawn. Slow load transitions with high peak values are representing a general quality change in greater patches of the lawn surface. This lawn type shows a very constant mowing progression. The density of the grass is evenly distributed with some discontinuity at the end of the track. That's why the results show low flickering and only two high and some smaller load transitions.

In the first two seconds of the track the mower is travelling over lawn ground with the travel drive on but with no grass to mow. The graph shows a slightly elevated high idle section with around 2750 rpm and 3 Nm. The main part consists of a constant mowing force with only a few smaller load shifts to 9 Nm. At the end of the track the lawn varies in quality so two clear peaks of load can be spotted in second 28 and 34. These load shifts can also be observed very well in the engine speed graph. Moreover the cutting torque in average is around 6.8 Nm which can be read in the histogram and gauss plot in Figure 15. Additionally the torque is showing a lot of fast load transition with low amplitude and its SD is around 1.5 Nm. This represents a stable and constant cutting force. The peak values at the end of the recording are reaching up to 11 Nm. Some discontinuous patches in the lawn surface are the cause for that. Over the main part of the recording the engine speed is oscillating around 2700 rpm with a mean value slightly

above 2700 rpm, as is presented in Figure 16. Corresponding to the load transitions the engine speed rises and falls. This can be observed in the second part of the speed graph in Figure 14. The course of the throttle position graph is displaying little throttle flap movement. The main value, which is drawn in Figure 17 is around 23 %TPS of WOT. The maximum throttle position is at about 50 %TPS at high loads.

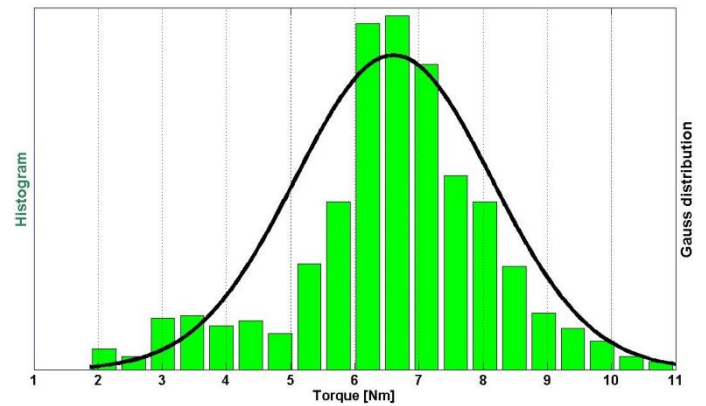


Figure 15: Torque distribution on turf lawn

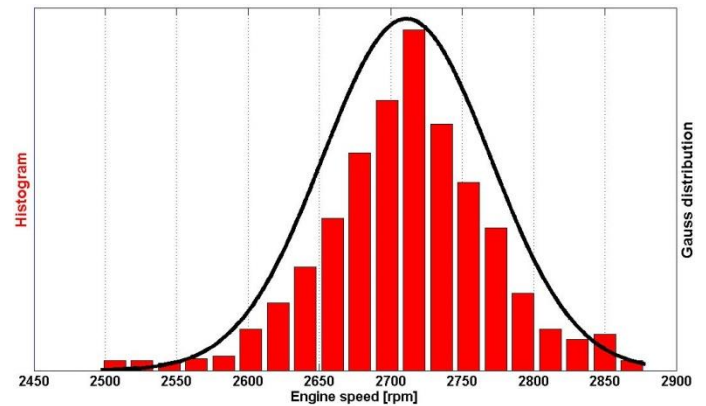


Figure 16: Engine Speed distribution on turf lawn

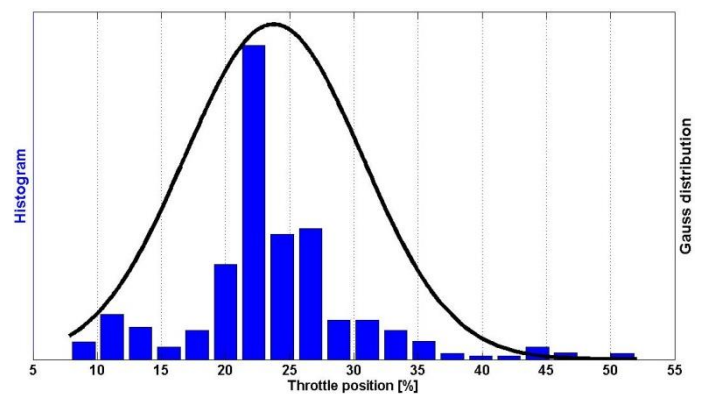


Figure 17: Throttle position distribution on turf lawn

In Figure 18 the load point distribution on turf lawn is shown. Engine torque over engine speed is printed with each circle representing the average value of one engine cycle or two engine revolutions respectively. As mentioned above the main load is sited between 2650 to 2780 rpm and 6 to 8 Nm (see concentration of indicators).

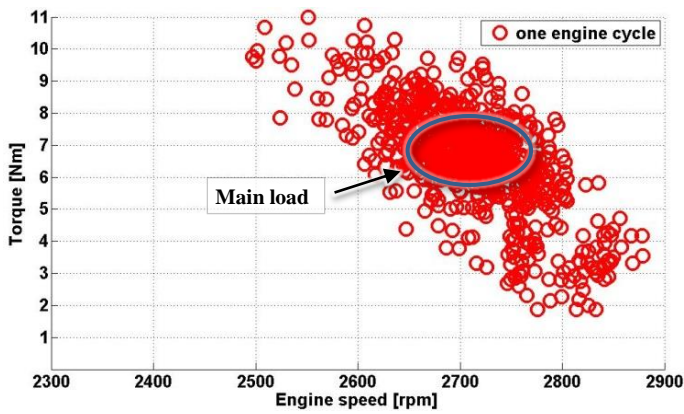


Figure 18: Load point plot on turf lawn

In Figure 19 the throttle position in % over the engine speed in rpm is displayed. Again, one circle represents one engine cycle. In black dashed lines the sequence of the TPS points is indicated. A best fit line is added to illustrate the average requirement of throttle flap movement on this lawn type. The main values for the throttle position lie between 20 %TPS and 28 % TPS. The two peak loads near the end of the track are clearly visible. They are represented through the two circle shaped tracks in the upper left corner. With lower throttle position and rising cutting force the engine speed drops. As a result the governor mechanism is opening the throttle flap to around 50 %TPS. Thereby the engine output increases and the engine speed is elevating again. The steepness and the direction of the tracks and hence the best fit line are representing the governor reaction speed. In this example the average demand of flap movement is at 8.37 °TPS per 100 rpm meaning ± 0.167 °TPS per engine cycle. The maximum throttle flap opening value, which is reached in the last great load peak, reaches 5.42 °TPS per engine cycle. At an engine speed of 2500 rpm this results in 112.9 °TPS per second.

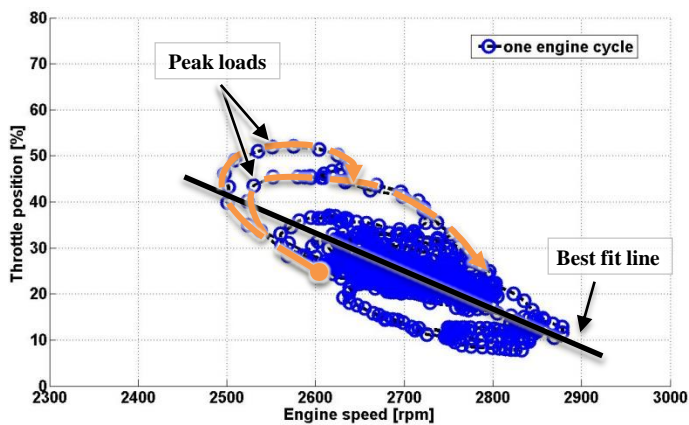


Figure 19: Throttle position plot on turf lawn

Farm grassland 8 – 12 cm, 3rd gear, 4 cm cutting height:

In Figure 20 the record of the farm grass land test is displayed. It shows obvious differences to the turf lawn experiment. Even though the average torque value is also around 7 Nm, the fast fluctuation of the load is much stronger. The SD is roughly ± 2.5 Nm. There are no explicit

load peaks and therefore no significant engine speed variations or throttle movements. An explanation for this could be that the distribution of grasses is well balanced and the density is not as high as for the turf lawn. Furthermore, the number of coarse and strong herbage stems is higher, whereas turf lawn mainly consists of leaves. As a result the cutting force is fluctuating. These short but high load requirements are covered by the inertia of the engine and the cutting blade with the engine speed showing no big drops but generally being kept lower.

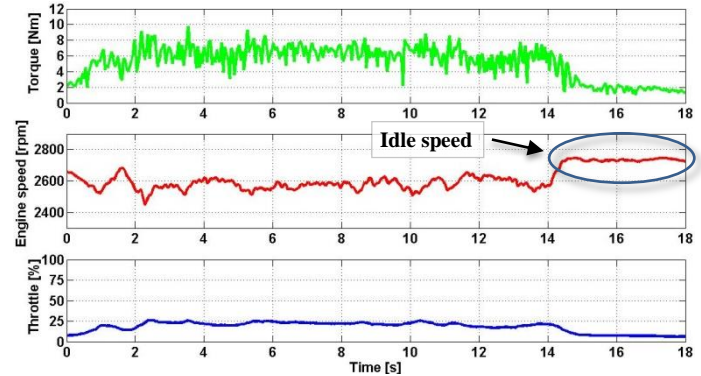


Figure 20: Cutting torque, engine speed and throttle position on farm grassland

As can be seen in the load distribution plot in Figure 21, the average engine speed on this surface is lower than on turf lawn, with 2540 rpm to 2620 rpm. Moreover the main load is sited between 5 Nm and 8 Nm. The round shape and loose spread of the load points display the wide range of fast load fluctuation. In the lower right sector the accumulation represents the idle section at the last 3 seconds of the track. This idle state is located in the area of 2740 rpm and 1.8 Nm.

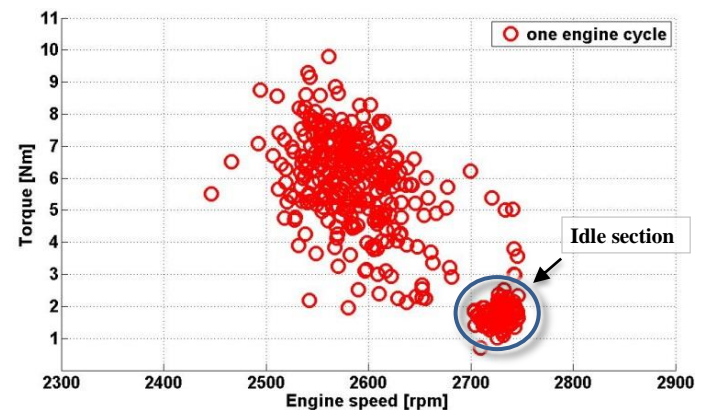


Figure 21: Load point plot on farm grassland

The throttle position plot (Figure 22) clearly depicts the above explained. The data analysis results in an average value of 22 %TPS. Moreover the idle speed throttle angle is around 7 %TPS. This idle section is also represented in the lower right corner with a higher engine speed and lower throttle angles.

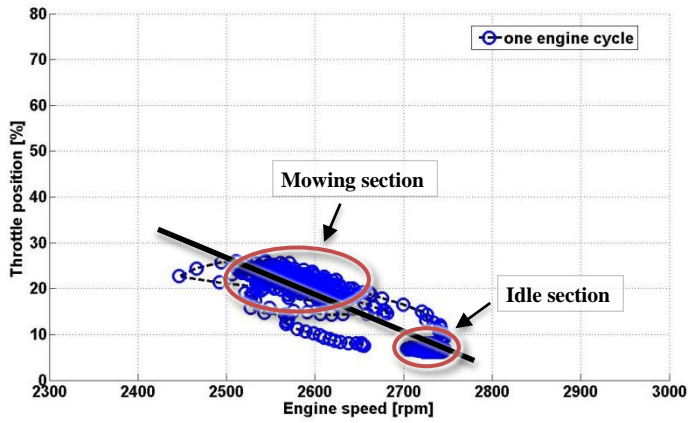


Figure 22: Throttle position plot on farm grass land

The following findings from the calculation of the best fit line can be summarised. The gradient of the best fit line is at 8.05°TPS per 100 rpm respectively $\pm 0.161^{\circ}\text{TPS}$ per engine cycle which is slightly lower than on turf lawn. This means that the throttle movement requirement is not as high as for turf lawn surface which can be seen in Figure 20. The maximum throttle flap opening value, which is reached in the first two seconds of the recording, reaches 1.46°TPS per engine cycle. At an engine speed of 2500 rpm, 30.4°TPS per second are achieved.

High meadow 50 cm, 1st gear, 7 cm cutting height:

A high meadow as is used in this experiment is a rough environment and for sure represents the upper end of the load scale for this lawnmower. That is why the test run is performed using the lowest gear and the highest cutting height.

Analysing the output data of the test on high meadow, one can make the following statements. The average load is slightly higher than at the other surfaces, with 5.5 Nm to 8.3 Nm: The engine speed lies within the same range as on the turf lawn, ranging between 2650 rpm and 2750 rpm. The fast load fluctuations are also similar to the test on turf lawn but there are significantly more high load peaks and thus engine speed drops. Especially at the end of the test track there is a section with the engine speed dropping to 2400 rpm and a throttle position of up to 75 %TPS.

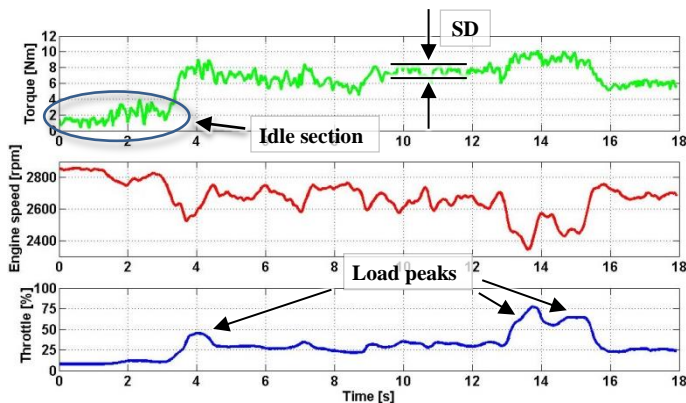


Figure 23: Cutting torque, engine speed and throttle position on high meadow

This is caused by bunches of rough weed in the lawn. The two explicit load peaks produced show the engine behaviour during intense load transition very well. In Figure 24 and in Figure 25 the drop of the engine speed through elevated cutting force is pictured well. It can be expected that the engine would stall if the load wouldn't ease off. In real life usage the user probably would react accordingly in order to keep the mower from stalling, for example by retracting or slightly lifting it off the lawn.

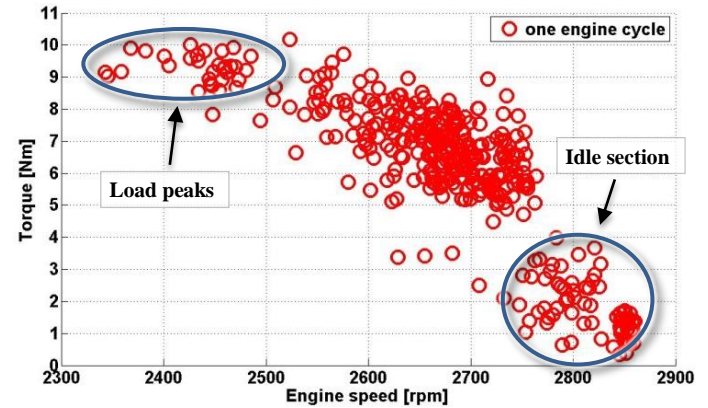


Figure 24: Load point plot on high meadow

In Figure 25 the tracks of the three distinctive load peaks can be pursued. The first one at second 4 is displayed in the smaller cycle around the centre of the spread. The second and third which are located around second 14 are starting out of the pointer cloud in the centre in direction of the upper left corner. After the load easing off a bit at 2450 rpm and 60 %TPS the track is heading on to the upper left corner with values up to 2350 rpm and 75 %TPS. The rising engine output is pushing up the speed again. Simultaneously the governor system closes the throttle flap. The next load peak is cutting down the velocity once more. After another opening of the throttle flap the track completes the middle circle and drops back to the indicator cloud.

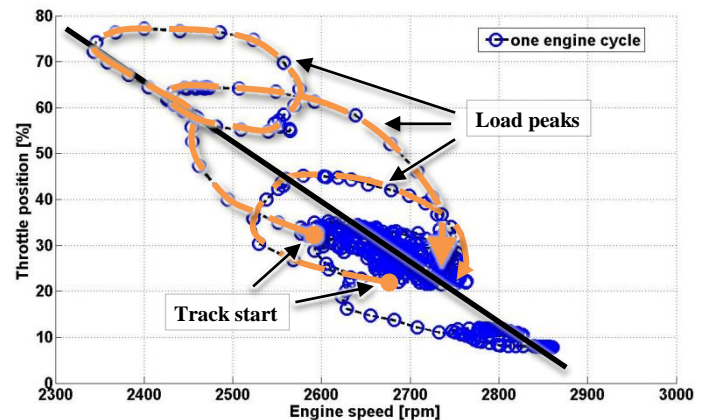


Figure 25: Throttle position plot on high meadow

The evaluation of the best fit line yields an average gradient of 13.17°TPS per 100rpm respectively 0.263°TPS per one engine cycle. The maximum governor deviation speed located at second 13 and reaches 7.31°TPS per engine cycle. At an engine speed of 2550rpm this results in 155.5°TPS per second. This is clearly the highest value achieved.

General results of the real world tests:

Combustion centre

It is well known, that for best efficiency the centre of combustion of four stroke gasoline engines is around 8°CA after top dead centre [7]. For now CTDC is defined as 0°CA . As can be seen in Figure 26, the average value of the test on turf lawn is at approximately 22°CA . This is a late setting and caused by the ignition system which is fixed to a specific crank angle position. In idle speed the values reach 40°CA and only at the highest load peaks the values are close to the optimum. This combustion behaviour induces thermodynamic losses. They are caused by the shift of the energy conversion process from a constant-volume cycle to a constant-pressure cycle, which is less the ideal process for a gasoline engine.

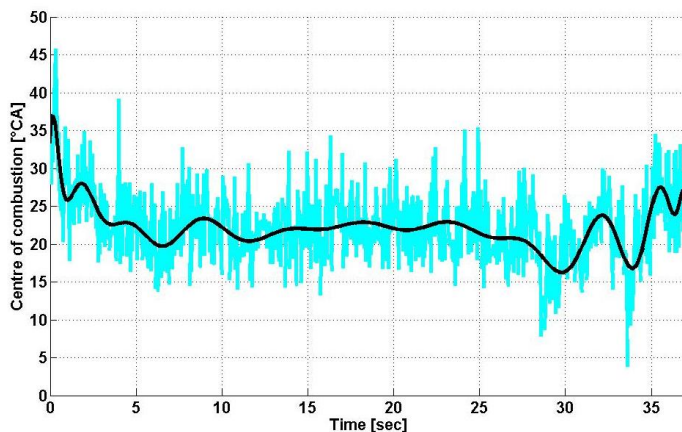


Figure 26: Centre of combustion on turf lawn

Lambda value

The optimum lambda setting for maximal engine performance is at around 0.9 [8]. When using a three way exhaust gas catalyst, the setting needs to be adjusted to lambda 1, respectively an air to fuel ratio of 14.7. In Figure 27 the lambda value over time on turf lawn is depicted. It shows that, with the given carburettor setting, a lambda value near 0.9 is reached only in idle state. At higher loads a very rich setting can be spotted. Especially at high load transitions when the throttle flap quickly opens to a wide angle, distinctive mixture enrichment can be observed. The values are dropping to lambda 0.65. The peak shortly after second 29 in Figure 28 matches with throttle flap opening in Figure 29.

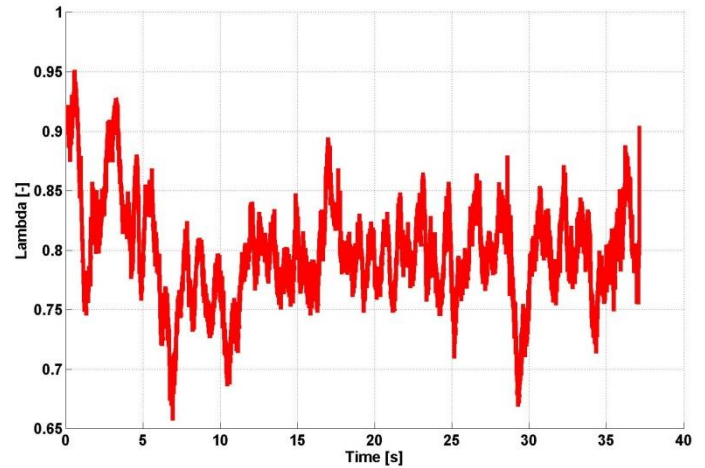


Figure 27: Lambda graph on turf lawn

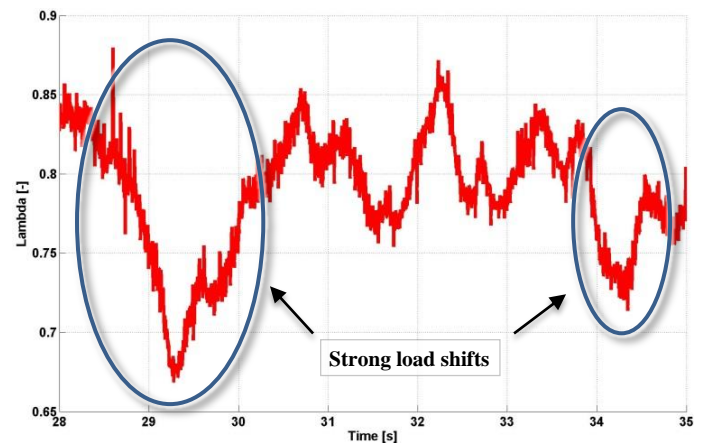


Figure 28: Lambda graph on turf lawn, zoom in on 28 to 35 seconds

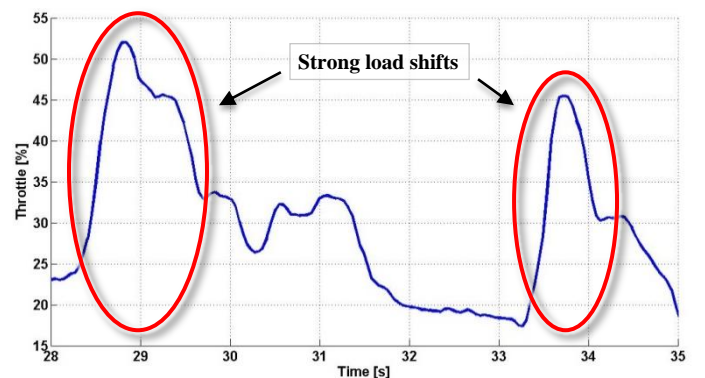


Figure 29: Throttle position on turf lawn, zoom in on 28 to 35 seconds

The histogram and gauss distribution plot in Figure 30 shows an average lambda value of the complete test run on turf lawn of 0.78. The main amount of the values is positioned between 0.75 and 0.81.

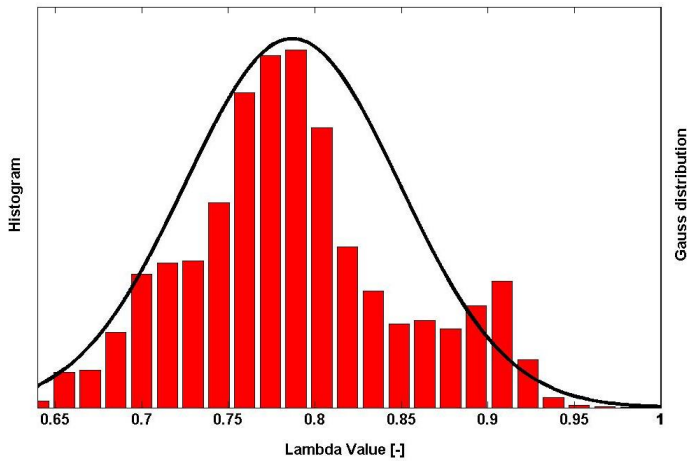


Figure 30: Lambda distribution on turf lawn

Idle speed

The idle load point on lawn with operating wing blade is at 1.8 Nm and 2800 rpm in average. High idle states, when the travel drive is used, can reach values of 3 Nm.

In addition there were carried out idle state test in standstill with operating blade and highest cutting position on asphalt surface. The results are:

1. Mulching blade: 2800 rpm / 0.55 Nm
2. Wing blade: 2800 rpm / 1.66 Nm

TEST BENCH INVESTIGATIONS

Getting a comprehensive overview about the engine characteristics is the target of the test bench investigations clarified in the following section. Additionally to the real world tests, complete engine maps of the above discussed engine values including data of engine out emissions and fuel consumption are acquired. This is crucial for enabling the interpretation of the engine behaviour and making predictions for future use.

Basic measurement categories for this experiment are explained in the chapter *real world tests*. Additional parameters are:

Measurement categories

1. Intake and exhaust gas temperature

A thermocouple type k sensor is used to detect the intake air and exhaust gas temperature.

Type K (NiCr / Ni)

Class 2: $\pm 2.2 \text{ }^\circ\text{C}$ or $\pm 0.0075 \text{ }^\circ\text{C}$

Manufacturer: RS components

2. Fuel mass flow

The fuel mass flow data is provided by an inside gear measurement system especially designed for very small fuel flows.

AVL Sore PLU 110

Measurement uncertainty: 0.2 %

Flow measurement range: 0.1 - 20 l/h

Manufacturer: AVL List GmbH

3. Engine-out emissions via CVS system

The exhaust gas composition is detected via a CVS system including an emission analyser.

AVL AMA i60

Linearity: $\leq 2 \%$

Manufacturer: AVL List GmbH

4. Engine torque:

The engine torque is measured via a torque measuring flange.

Kistler 4504A

Accuracy class: 0.1

Manufacturer: Kistler GmbH

In engine design some specific values have been established which are convenient for comparing different engine types. They are applied in legislation directives or specification documentation. For example: Brake Specific Fuel consumption in g/kWh or engine-out emissions in g/kWh. Measurement data is the basis for their calculation.

ENGINE TEST BED MOUNT

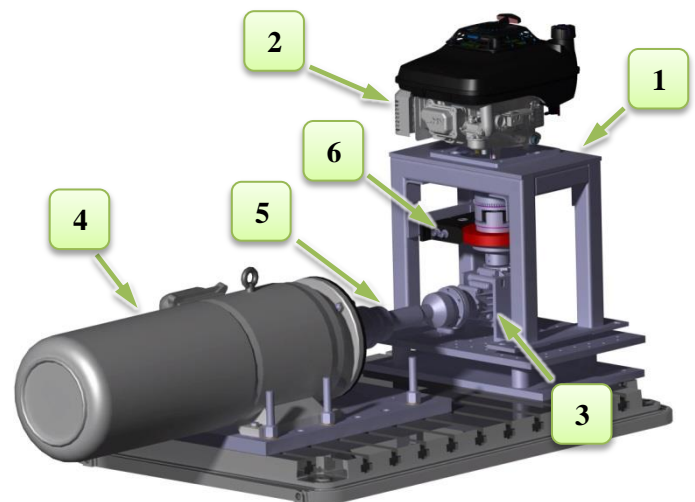


Figure 31: Test bench design in CAD

The CAD model in Catia V5 is shown in Figure 31. First the engine test bed mount (1) needs to be designed and constructed. The engine (2) requires the original mounting position. For this purpose a 90 degree gearbox (3) with a transmission ratio of 1 is used for the coupling to the asynchronous motor which is serving as test bed brake (4). A cardan shaft (5) is placed between the gearbox and the brake for an easier positioning of the gearbox. The torque sensor (6), is mounted between the gearbox and the engine. Furthermore a rubber element torsion damping clutch is set directly on the crank shaft. It reduces the torque peaks produced by the single cylinder which otherwise would lead to mechanical problems in the measurement instrumentation or the drivetrain.

EXPERIMENT AND RESULTS

For the preparation of the engine map the measurement grid needs to be configured. First the lower and the upper engine speed limits are defined at 1600 rpm and 3000 rpm. Then the pitch of the engine speed between the borders is set. In this case it is 200 rpm. After that the full-load curve is measured in the predefined steps. Again with the obtained values of the torque a pitch for the load is set. Using this specified pattern, the engine is set to each load point by defining the speed via the brake revolutions and the torque by means of the throttle valve position. This is called the M/α control. After the measuring quantities have levelled a measurement is started. In the end the sum of the grid points can be plotted in different ways to analyse the engine characteristics.

Hereinafter numerous results of the test bench investigations are presented. The findings are displayed in engine maps where the engine torque in Nm on the y-axis is drawn over the engine speed in rpm on the x-axis. In the z-axis direction the values of different analysis categories are depicted. Lines of constant values are displayed in black.

Brake specific fuel consumption

First the brake specific fuel consumption is assessed. Its engine map is depicted in Figure 32. The BSFC value describes the fuel consumption in relation to the engine output. This represents a certain degree of efficiency. Dots in the grid show the position of each measuring point. Green colours areas representing areas with low values and red colours areas with high values (at black and white print green is pictured in light grey and red in dark grey). The BSFC engine map shows values between 800 g/kWh at 2 Nm and 440 g/kWh at 7 Nm. The area of highest efficiency is located between 6 to 8.5 Nm and 1800 to 2600 rpm. There are two top points which show values of 438 g/kWh at 2400 rpm and 7 Nm and 1800 rpm and 6.5 Nm. According to the Kawasaki engine documentation [9] a value of 340 g/kWh is given. But it is to say that this value is documented for the original carburettor setting. Nevertheless the measured data is verified with a second mass flow system and a backup torque measurement flange.

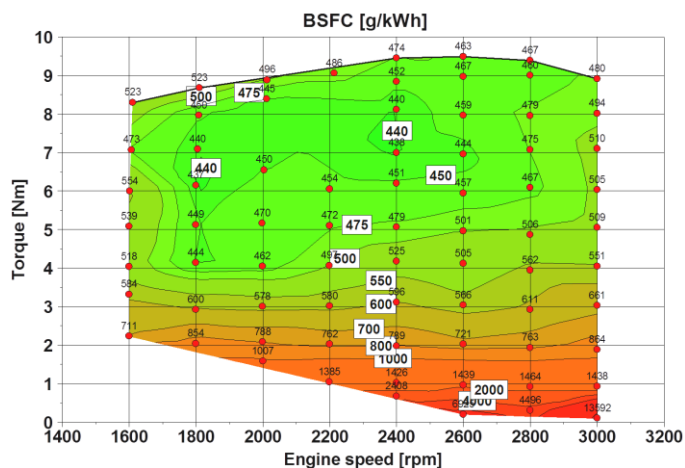


Figure 32: BSFC engine map

Lambda

In Figure 33 the lambda factor allocation is presented. Blue areas represent the leaner end of the scale and red areas the richer one (again at black and white print red is pictured in light grey and blue in dark grey). Generally the carburettor characteristic is set to a low lambda value. Over the mayor part of the engine map it is located around 0.8. In full load and in idle state it enriches down to 0.7. Comparing the above shown BSFC plot to the lambda plot, one can see the impact of the rich setting of the mixture ratio on the fuel consumption.

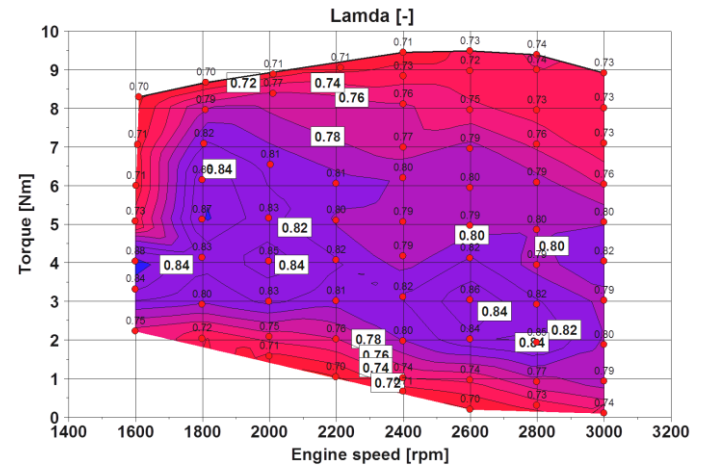


Figure 33: Lambda value engine map

Engine-out emissions

Engine-out emission behaviour also correlates with the above discussed, which shows through the following analysis. According to Figure 34 (with the same colour setting as in Figure 33), mixture enrichment goes hand in hand with high specific CO emissions. A lack of oxygen in the cylinder leads to an incomplete combustion resulting in high CO emission numbers and a loss of efficiency.

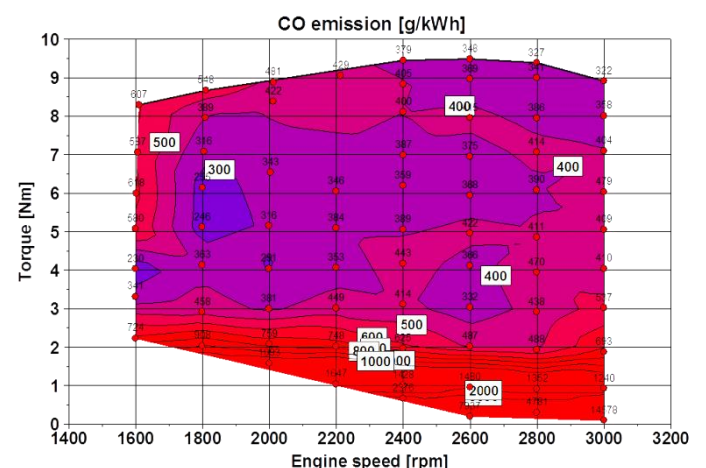


Figure 34: Specific CO emissions engine map in g/kWh

The emissions lie around 400 g/kWh over the main area of the engine map. In a small region around 6 Nm and 1800 rpm the best point is reached with 250 g/kWh but especially at idle conditions the CO emissions are reaching

very high values. One reason for this is that not only the absolute CO emissions are higher in idle state, but also the low engine power output is elevating the specific value.

In Figure 35 the NO_x emission distribution within the engine map can be read. It clearly accords with the findings mentioned before and with the ignition setting discussed in Figure 37. The values are around 2 g/kWh over the main parts of the engine map which is printed in blue (dark grey) colours. Only around 6 Nm and 1800 rpm there is a slightly elevated region drawn in red (light grey) with values up to 6 g/kWh. The early combustion centre in combination with the higher lambda values near 0.87 result in higher peak cylinder pressures and higher combustion temperatures. At the rest of the engine map the conditions for the endothermic NO_x reactions are not given.

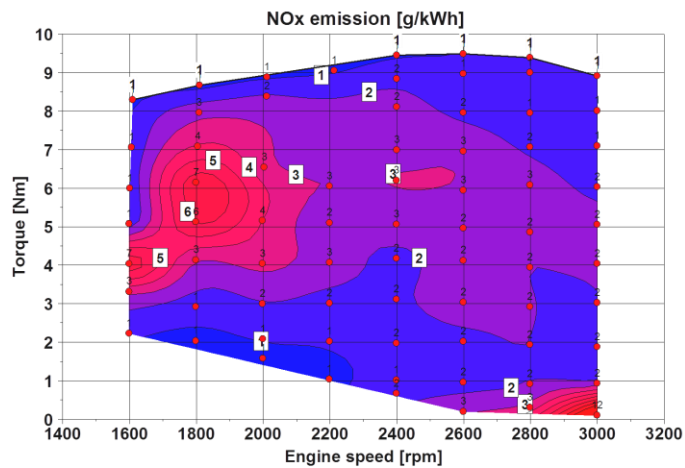


Figure 35: Specific NO_x emissions engine map in g/kWh

The HC emissions, based on CH₂, show values around 2 to 3 g/kWh except in the region with low engine power output.

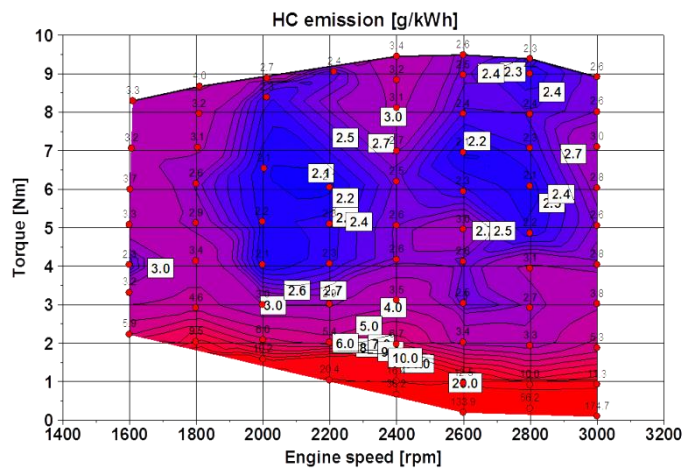


Figure 36: Specific HC emissions engine map in g/kWh

Another important engine parameter, as discussed in *General results of the real world tests*, is the centre of combustion. The 50 %MFB number spread can be looked up in Figure 37. With the actual setting the range of the fixed CDI is fully used. At around 1800 rpm and 7.5 Nm the combustion centre lies at 6 °CA after top dead centre, which

is seen as a limit for maximum efficiency. Stepping up the engine speed and lowering the load, the combustion centre is shifting to later angles until 40 °CA after TDC in 2800 rpm and 1 Nm is reached. Herein the disadvantages of the fixed ignition are clearly shown.

There are two main reasons for this behaviour. The first one is that with higher engine speed the timespan for the combustion to finish is getting smaller, so the centre moves to a later position. The second one is that with lower load the intake port velocity is decreasing which slows down the flame propagation velocity because of less in-cylinder turbulence [10].

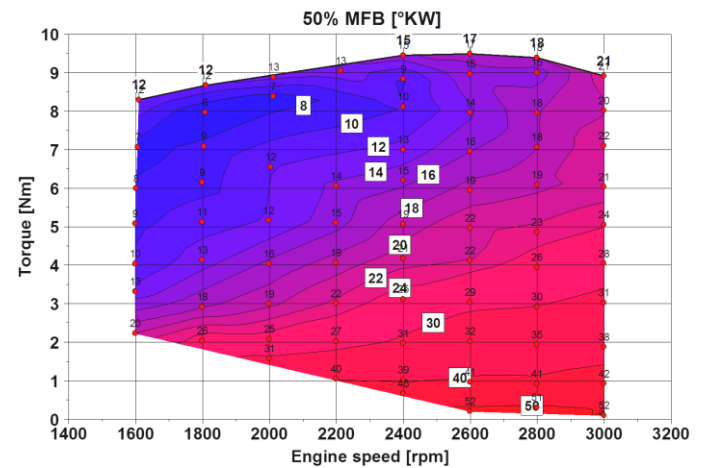


Figure 37: Ignition timing, 50 %MFB engine map

Engine characteristics

When plotting the engine load point distribution, as is described in detail in

Results of the real world test

over the engine map, the engine characteristics can be assessed. In Figure 38 load point distribution on turf lawn is drawn into the BSFC engine map. So one can clearly see where in the engine map the lawnmower is operating during real world usage.

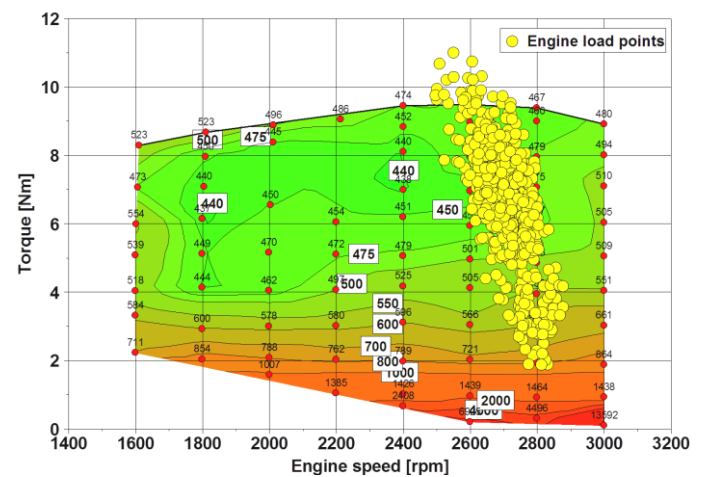


Figure 38: BSFC engine map with engine load points on turf lawn

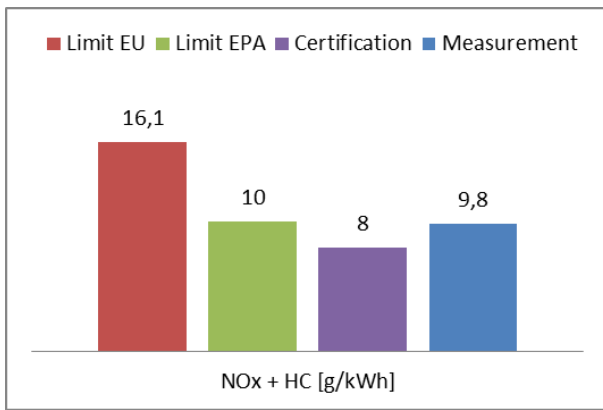


Figure 41: Comparison of the NOx + HC emission values

For the US market this engine has to be certified according to the CEPA air resource board emission directive [2]. The test cycle and the calculation procedure is the same as for the EU directive. In Figure 40 and Figure 41 these certification values are compared to the measurements and the legislation limits.

SUMMARY

Load distribution

The most frequently load points while mowing:

- 2600 – 2750rpm
- 6 – 8Nm
- 20 – 25%TPS

Load peaks: 2400rpm, 11Nm, 75%TPS
 High idle: 2750rpm, 3Nm, 12%TPS
 Standard idle: 2800rpm, 1.8Nm, 7%TPS

Flyweight governor

The reaction speed of the flyweight governor for most torque shifts is sufficient. Response on very fast load transition is damped due to the flyweight inertia. Small and fast load transitions are not covered with this mechanical system.

Maximum gradient: 13.2 °TPS per engine cycle

Carburettor

In general the carburettor characteristic is on the rich side. At transient operation the lambda values are alternating strongly. Fast load shifts result in an intense enrichment of the mixture.

- Transient operation lambda value

Mean value: 0.79
 Main range: 0.74 – 0.83
 Minimum: 0.64
 Maximum: 0.94

- Engine map lambda value

Mean value: 0.77
 Minimum: 0.7
 Maximum: 0.87

Combustion behaviour

The centre of combustion during mowing operation in general is rather late. The non-variable ignition system causes the 50% MFB point to move with engine speed and engine load. In the engine map this situation is clearly reflected.

Mean value: 22 °CA
 Minimum: 6 °CA
 Maximum: 51 °CA

Engine-out emissions

The engine-out emissions reflect the lambda values and the combustion behaviour. High CO values are reached as a cause of the low lambda. NOx is the critical criterion for the emission certification. Therefore values are kept low through the late combustion centre and the rich lambda setting. HC emissions are also low. As a result the emission legislation limits can be met.

CO mean: 425 g/kWh
 Minimum: 246 g/kWh
 Maximum: ~ 1500 g/kWh

NOx mean: 2.1 g/kWh
 Minimum: 0.7 g/kWh
 Maximum: 6.7 g/kWh

HC mean: 3.05 g/kWh
 Minimum: 2.1g/kWh
 Maximum: ~ 10 g/kWh

Brake specific fuel consumption

Efficiency correlates with the low lambda values and the late centre of combustion.

Maximum value: ~ 1000 g/kWh
 Minimum value: 438 g/kWh

Engine characteristics

The analysis shows that the engine setting for European markets is not ideal. Originally the engine is designed for idle state at 3200 rpm, consequently a mowing speed of about 3100 rpm. At this setting the power output is much higher as is the rotational inertial energy. Furthermore the cutting load is located clearly above the speed of the highest torque value. Thus the persistent high loads are countervailed through the engine torque reserves. At the European setting the engine has not enough torque compensation ability. The load demands for the first transient load points, which are overshooting the stationary

full load line are covered through the inertia of the engine and the cutting blade; if the load persists the engine stalls.

CONCLUSION

According to the CEPA certification, this engine has a life span of 500 hours. This is achieved through mixture enrichment (lower engine temperature), relatively low compression ratio plus late centre of combustion (low maximum cylinder pressure) and engine design (circular lubrication, steel camshaft). The analysis of the real world cycles shows distinct load point agglomeration, in idle state around 2800 rpm and 1.8Nm and while mowing at around 2700 rpm and 7 Nm. Maximum efficiency values are achieved at high cutting forces and can reach up to 19.5%. At part load or idle state, because of the necessary throttling, late ignition and rich mixture, the efficiency is considerably lower and lies at about 8.5%. Using a simple two stage switch ignition or an electronic CDI system could provide improvement to this situation. At moderate cutting force transition the flyweight governor reaction is sufficiently responding, but at fast and intense load shifts a more rapid response is wanted. As a consequence of this, only a part of the maximum power can be used, around 2.5 kW of 3.4 kW. An improved load control could shift the throttle characteristics to the area of higher torque output and engine speed. Using this potential could enable the reduction of the engine displacement, subsequently enhancing the efficiency in part load operation. For a four stroke engine of this size, the engine-out emission level of HC and NO_x is quite low. The lambda characteristic of the carburettor shows average values of 0.79. As the CO emissions mainly depend on the lambda setting, they reach as expected, high values. By implementing this strategy the engine is able to fulfil the emission legislation limits for European and US markets. A leaner mixture could reduce CO emissions and simultaneously rise the degree of efficiency. As a consequence of the trade-off between BSFC and NO_x emissions, without after gas treatment or other technical measures it's difficult to fulfil the legislation limits of NO_x. An implementation of EGR could provide a possible solution to this problem.

For tools like this lawnmower, ICE's will still be the main propulsion type, whereas there is noticeable competition from electrification. Therefore an improvement of the degree of efficiency and an engine out and noise emission reduction should be aspired. The lambda value and ignition timing are showing the greatest potential for this. Furthermore changes in the engine design, after gas treatment or EGR could be required. For being able to handle all these challenges, further research will be indispensable.

LIST OF REFERENCES

- [1] Kawasaki Engines Europe N.V., "http://www.kawasaki-engines.eu/de," Kawasaki Engines Europe N.V., 2013. [Online]. Available: http://www.kawasaki-engines.eu/de/engines/FEB567116/FJ180V_STD. [Accessed 03 2013].
- [2] California Environmental Protection Agency Air Resources Board, "http://www.arb.ca.gov/homepage.htm," 26 07 2004. [Online]. Available: <http://www.arb.ca.gov/msprog/offroad/sore/sorectp/sorectp.htm#reg>. [Accessed 25 04 2013].
- [3] THE EUROPEAN PARLIAMENT AND THE COUNCIL, *DIRECTIVE 2000/14/EC OF THE EUROPEAN PARLIAMENT AND OF THE COUNCIL*, 2000.
- [4] H. M. Y. S. Y. T. Tomoki Fukushima, "Governor System for General Purpose Engine Using Adaptive Control Theory," *SETC*, no. 2006-32-0008, 2006.
- [5] Kawasaki Heavy Industries Ltd., Service Manual FJ180V, 08 2010.
- [6] Viking GmbH, "www.viking.at," Viking GmbH, 2013. [Online]. Available: <http://www.viking.at/VIKING-Produkte/Rasenm%C3%A4her/Rasenm%C3%A4her-f%C3%BCr-den-professionellen-Einsatz/21740-1517/MB-750-KS.aspx>. [Accessed 03 2013].
- [7] R. Pischinger, M. Klell und T. Sams, *Thermodynamik der Verbrennungskraftmaschine*, Springer, 2002.
- [8] H. Eichlseder, M. Klütting and W. F. Piock, *Grundlagen und Technologien des Ottomotors*, Springer Wien New York, 2008.
- [9] Kawasaki Motors Europe N.V., "www.kawasaki-engines.eu," 10 2011. [Online].
- [10] G. P. Merker and C. Schwarz, *Grundlagen Verbrennungsmotoren*, Vieweg+Teubner, 2009.
- [11] European parliament and council, *DIRECTIVE 97/68/EC OF THE EUROPEAN PARLIAMENT AND OF THE COUNCIL*, 16/12/1997 .

CONTACT INFORMATION

Hermann Edtmayer
E-mail: edtmayer@ivt.tugraz.at
Phone: +43/316 873 30155

Alexander Trattner
E-mail: trattner@ivt.tugraz.at
Phone: +43/316 873 30165

Stephan Schmidt
E-mail: schmidt@ivt.tugraz.at
Phone: +43/316 873 30153

Roland Kirchberger
E-mail: kirchberger@ivt.tugraz.at
Phone: +43/316 873 30150

Graz University of Technology
Institute of Internal Combustion Engines &
Thermodynamics
Research Area Design
ECO-PowerDrive
Inffeldgasse 25B
8010 Graz – Austria

Jakob Trentini
E-mail: jakob.trentini@viking.at
Phone: +43/5372 6972 308

Johann Weiglhofer
E-mail: johann.weiglhofer@viking.at
Phone: +43/5372 6972 266

Viking GmbH
Hans Peter Stihl-Straße 5
6336 Langkapfen/Kufstein – Austria

ACKNOWLEDGMENTS

The author would like to thank all the team members for their work committed in this research project. Special thanks to the research partner Viking for providing technical equipment, company staff and the test facility.



DEFINITIONS/ABBREVIATIONS

ICE...	Internal combustion engine
ECU...	Engine control unit
EMS...	Engine management system
CDI...	Capacitor discharge ignition
MFB...	Mass fraction burned
IMEP...	Indicated mean effective pressure
BMEP...	Brake mean effective pressure
WOT...	Wide open throttle
TPS...	Throttle position
CA...	Crank angle
TDC...	Top dead centre
CTDC...	Combustion top dead centre
CVS...	Constant volume sampling
BSFC...	Brake specific fuel consumption
CEPA...	California environmental protection agency
EGR...	Exhaust gas recirculation
SD...	Standard deviation